PREPRINT

Not Peer Reviewed

RESEARCH ARTICLE

A *COEAE80* esterase variant and P450-suppression drive chlorfenapyr resistance in malaria vectors

[version 1]

Magellan Tchouakui[1], Carlos S. Djoko Tagne[1,2], Hervé R. Tazokong[1,3], Jonas A. Kengne Ouafo[1], Mersimine Kouamo[1], Derrick Fofie[1,4], Arnaud Tepa[1,5], Murielle Wondji[1,6], Sulaiman S. Ibrahim[1,7], Charles S. Wondji[1,6]

[1]Medical Entomology, Centre for Research in Infectious Diseases, Yaounde, cENTRE, 13591, Cameroon
[2]Department of Biochemistry, University of Bamenda, Bamenda, 39, Cameroon
[3]Department of Microbiology, University of Yaoundé, Yaounde, cENTRE, 812, Cameroon
[4]Department of Animal Biology and Physiology, University of Yaoundé 1, Yaounde, cENTRE, 812, Cameroon
[5]Faculty of Medicine and Biomedical Science, University of Yaoundé 1, Yaounde, cENTRE, 812, Cameroon
[6]Department of Vector Biology, Liverpool School of Tropical Medicine, Liverpool, Pembroke Place, L35QA, UK
[7]Department of Biochemistry, Bayero University, kano, Kano, PMB 3011, Nigeria

v1 **First published:** 31 Oct 2025, **2**:355
https://doi.org/10.12688/verixiv.2295.1

Latest published: 31 Oct 2025, **2**:355
https://doi.org/10.12688/verixiv.2295.1

Abstract

Chlorfenapyr (CFP)-treated nets are currently the most efficacious malaria vector control tools. Anticipating the development and mechanisms of resistance is vital to prolonging their effectiveness. Here, we demonstrate that the E510D mutation in the overexpressed carboxylesterase *COEAE80*, coupled with CYP450s suppression confer CFP resistance in *Anopheles gambiae.* Multi-omics analyses identified the transcriptional signatures of CFP resistance with *COEAE80* up-regulation and a marked down-regulation of the major P450s associated with pyrethroid resistance. Whole genome sequencing detected signatures of selective sweep around *COEAE80* and functional genomics validation confirm it confers CFP resistance. DNA-based genotyping revealed that 510D- *COEAE80* mosquitoes significantly survive CFP exposure, in contrast to E510-*COEAE80* mosquitoes and pyrethroid resistant E205D-*CYP6P3* individuals. The 510D allele was detected Africa-wide, calling for urgent measures to anticipate and counteract CFP resistance.

Keywords
malaria vector control, Chlorfenapyr (CFP)-treated nets, resistance mechanisms, carboxylesterase COEAE80, E510D mutation, CYP450 suppression, Anopheles gambiae

This article is included in the Gates Foundation gateway.

Corresponding authors: Magellan Tchouakui (magellan.tchouakui@crid-cam.net), Charles S. Wondji (charles.wondji@lstmed.ac.uk)

Author roles: Tchouakui M: Conceptualization, Data Curation, Formal Analysis, Investigation, Methodology, Resources, Supervision, Validation, Visualization, Writing – Original Draft Preparation, Writing – Review & Editing; **Djoko Tagne CS**: Investigation, Methodology, Writing – Review & Editing; **Tazokong HR**: Data Curation, Formal Analysis, Investigation, Methodology, Software, Writing – Review & Editing; **Kengne Ouafo JA**: Data Curation, Formal Analysis, Investigation, Methodology, Software, Writing – Review & Editing; **Kouamo M** : Formal Analysis, Investigation, Methodology; **Fofie D**: Investigation, Methodology; **Tepa A**: Data Curation, Formal Analysis, Investigation, Methodology, Software; **Wondji M**: Investigation, Methodology; **Ibrahim SS**: Supervision, Writing – Review & Editing; **Wondji CS**: Conceptualization, Data Curation, Formal Analysis, Funding Acquisition, Project Administration, Resources, Software, Supervision, Validation, Visualization, Writing – Review & Editing

Competing interests: No competing interests were disclosed.

Grant information: This work was supported by the BMGF Grant (INV-006003) awarded to CSW. The views expressed in this publication are those of the authors and not necessarily BMGF.
The funders had no role in study design, data collection and analysis, decision to publish, or preparation of the manuscript.

How to cite this article: Tchouakui M, Djoko Tagne CS, Tazokong HR *et al.* **A *COEAE80* esterase variant and P450-suppression drive chlorfenapyr resistance in malaria vectors [version 1]** VeriXiv 2025, **2**:355 https://doi.org/10.12688/verixiv.2295.1

First published: 31 Oct 2025, **2**:355 https://doi.org/10.12688/verixiv.2295.1

Editor's summary

Chlorfenapyr (CFP)-based bed nets are currently the most efficient treated nets against pyrethroid-resistant malaria vectors, saving lives Africa-wide. However, it is crucial to anticipate resistance development to prolong their efficacy. Tchouakui et al utilized a multi-omics approach including RNA-Seq and Whole Genome Sequencing (WGS), followed by extensive *in-vivo*/*in-silico* functional validation to identify genes and genetic variants conferring CFP resistance in laboratory-selected *Anopheles gambiae* mosquitoes. Major metabolic genes conferring pyrethroid resistance were down-regulated in CFP-resistant samples, while over-expressed genes included the carboxylesterase *COEAE80* linked with a signature of directional selection. A mutation, E510D-*COEAE80*, was shown to confer CFP resistance in both lab and field strains. This study provides the first characterization of the molecular basis of CFP resistance in malaria vectors and provides tools for early detection and resistance management.

Introduction

Malaria control efforts have significantly stalled since 2015 due to the intensification of resistance to pyrethroids, the key insecticide used for long-lasting insecticidal nets (LLINs) and indoor residual spraying (IRS).[1,2] Consequently, new generation LLINs combining pyrethroids with the new active ingredient Chlorfenapyr (CFP) e.g., Interceptor G2 (IG2) is now recommended by WHO, with a greater reduction of malaria incidence demonstrated in two randomized-controlled trials.[3,4] The CFP-based nets are currently being extensively rolled out across Africa to help reduce malaria burden.[5] However, such large-scale deployments will ultimately exert a selective pressure on mosquitoes and likely select for resistance, as it has been the case of the pyrethroid insecticides.[2] Therefore, understanding the speed of CFP resistance selection and elucidating the underlying mechanisms is paramount to design suitable strategies to delay the evolution of the resistance and to prolong the efficacy of these new tools.

Chlorfenapyr is a broad-spectrum pyrrole pesticide belonging to IRAC Group 13, previously mainly used for termite control and crop protection against a variety of insect and mite pests.[6–10] It was recently introduced in vector control to fight against the Anopheles mosquitoes.[6] It is a pro-insecticide which requires bioactivation to insecticidally toxic primary metabolite, tralopyril, by removing an N-ethoxymethyl group in a reaction catalysed by mixed function oxidases enzymes.[11,12] It is tralopyril which kills insects by disrupting energy production in the mitochondria by uncoupling oxidative phosphorylation. Although the detoxification or tolerance mechanism of several pests to chlorfenapyr have been investigated,[8,13–16] at present the molecular basis of chlorfenapyr resistance in major malaria vectors remain unknown, and molecular assays for chlorfenapyr resistance monitoring are lacking. As the mode of action of chlorfenapyr is completely different from that of standard neurotoxic insecticides, there is less expectations for cross–resistance issues. In field/lab pyrethroid-resistant *An. funestus* for example, we have seen high CFP susceptibility due the major pyrethroid resistance genes CYP6P9a/b (which are highly over-expressed across Africa) involved in its bioactivation into tralopyril[17] revealing cross negative resistance between these pyrethroids resistance markers and CFP. Unfortunately, little is known about the mechanism of the nascent CFP resistance reported in *An. gambiae* in some regions.[18] Previous studies on CFP resistance mechanisms had been done in some crop pests including in *Tetranychus urticae*[8] and in *Aphis glycines Matsumura*[19] using broad biochemical analysis suggesting a role of esterases although no specific genes were detected. A recent investigation of resistance mechanisms to CFP performed in the crop pest *T. urticae*, using a lab experimental selection approach and QTL mapping revealed that adaption was linked to downregulation of some prominent P450s known to confer resistance to another insecticide class (amitraz).[13] This study highlighted a complex mechanism of CFP adaption caused by reduced activation efficiency but failed to detect a molecular diagnostic tool for monitoring CFP in the field population of crop pest.[13] In the malaria vector *An. gambiae* key P450s (e.g. *CYP6P3*, *CYP9J5*, and *CYP9K1)* known to confer pyrethroid resistance have been shown to convert CFP into tralopyril[6] suggesting potential negative cross resistance between pyrethroid and CFP as observed previously in *An funestus.*[17] Identifying the molecular mechanisms of chlorfenapyr resistance in major malaria vectors such as *An. gambiae* will facilitate development of suitable molecular diagnostic assays for resistance monitoring and implementation of evidence-based resistance prevention and management strategies.

Here, to help prolong the effectiveness of CFP-based control tools, we artificially evolved CFP resistance using selection experiments in *An. gambiae* and elucidated the underlying molecular basis of the resistance, demonstrating that a single amino acid change in an alpha esterase *COEAE80* gene coupled with suppression of the expression of key pyrethroid-associated cytochrome P450s confers CFP resistance.

Results

Chlorfenapyr resistance was successfully selected in the laboratory

To predict the future development of chlorfenapyr (CFP) resistance in the field mosquitoes, a hybrid strain was created by crossing a field-collected *Anopheles gambiae* population from Cameroon, known to exhibit reduced CFP susceptibility,[6] with the laboratory-susceptible Kisumu strain. After 12 generations of selection with a diagnostic dose of CFP 100 µg/ml,

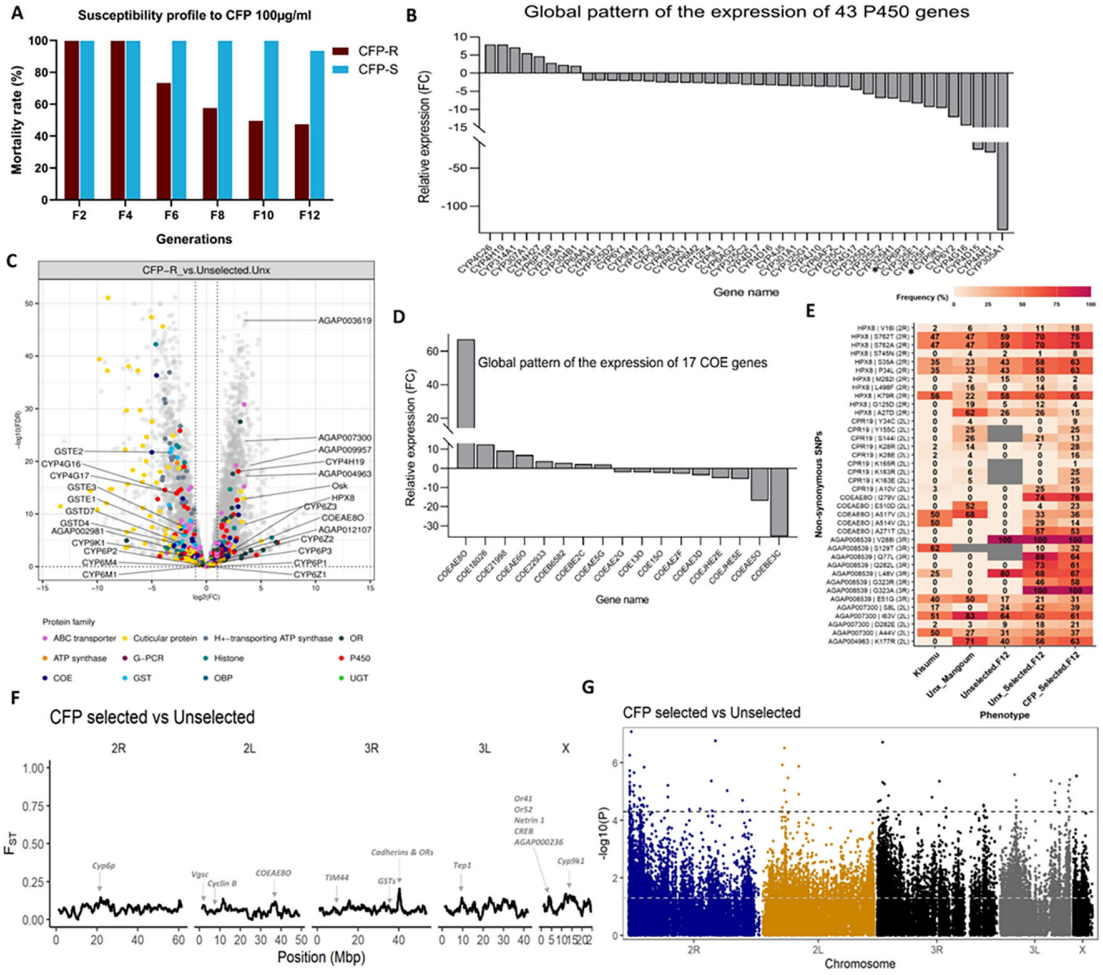

Figure 1. Transcriptomic profiling of chlorfenapyr resistance. (A) Resistance dynamics of various chlorfenapyr lines during the selection process; resistance levels were compared using CDC bottle assays and are expressed as mean % mortality from 5 replicates ± SEM. (B) Global expression profile of pyrethroid-associated cytochrome P450s in CFP-resistance mosquitoes compared to the unselected line. (C) Volcano plot of differential gene expression between F_{12} chlorfenapyr-resistant alive after exposure to CFP (CFP-R) and the unselected (unexposed). * The main pyrethroid resistance P450 genes *CYP6P3* and *CYP9K1* are significantly downregulated in CFP-R line vs Unselected line and have been shown by Yunta *et al.*[6] to bioactivate CFP to tralopyril. The vertical dotted lines indicate 2-fold change expression cut-off (absolute value), and the horizontal lines indicate an FDR of 0.05. OR: odorant receptor, G-PCR: G-Protein coupled receptors, P450: cytochrome P450s, COE: carboxylesterases, GST: glutathione-S-transferases, OBP: Odorant-Biding proteins and UGT: UDP-glucuronosyltransferases. (D) Global expression profile of carboxylesterases in CFP-resistance mosquitoes compared to the unselected line. (E) Allele frequency of key non-synonymous mutations from top upregulated genes of interest between study populations obtained after RNA-sequencing. CFP_Selected.F12: chlorfenapyr-selected F_{12} generation alive after exposure to CFP-100, Unx_Selected.F12: chlorfenapyr-selected F_{12} generation but unexposed, Unselected.F12: CFP susceptible unexposed from unselected line at F12 generation, Unx_Mangoum: unexposed parental strain from the field Mangoum and Kisumu: the susceptible lab strain Kisumu. (F) Genetic differentiation index (F_{ST}) between CFP_Selected.F12 and unselected unexposed. (G) Manhattan plot of the Welch's t-test results between CFP_Selected.F12 and unselected unexposed.

the selected line demonstrated a significantly reduced susceptibility (Figure 1A). The mortality rate decreased from 100% in the second generation (F_2) to 47.8 ± 4.6% at the twelfth generation (F_{12}) ($P < 0.0001$). In contrast, the unselected control line remained fully susceptible to the same dose of CFP, confirming the successful induction of CFP resistance in the selected line.

The marked up-regulation of the carboxylesterase *COEAE80* in chlorfenapyr resistant mosquitoes contrasts with an extensive downregulation of cytochrome P450s

RNA sequencing performed using F_{12} progenies generated more than 100 M reads across the four replicates for each line **(Data S2).** A comparative analysis between the selected (alive after exposure to CFP or unexposed) and the unselected

line at the 12th generation (F_{12}) detected marked differences in the expression of key candidate detoxification genes (Figure 1**, B, C** and **D,** and **Figure S1).** The carboxylesterase *COEAE80* (AGAP006700) was the main detoxification gene consistently over-expressed in mosquitoes that survived exposure to CFP (R) either when compared to unselected (S) (Fold-change = 67.1) (Figure 1, **C** and **D, Figure S1**and **Table S1)** or to those selected but unexposed to CFP (C) (FC = 2.3) **(Figure S1E,** and **Data S3** to **S5)** suggesting that this gene could play a major role in the resistance to chlorfenapyr. Other genes consistently overexpressed in the 3 comparisons included a heme peroxidase (*HPX8*, AGAP004038; FC = 24.2), a cuticular protein *CPR19* (AGAP005968), *Histone3* (AGAP012197), asparagine synthetase B (AGAP012923), and an ionotropic receptor, *Ir199* (AGAP029201) **(Data S3** to **S5)**. Since CFP kills insects by disrupting ATP production by mitochondria, genes associated with mitochondrial activities were specifically analyzed. The translocase of inner mitochondrial membrane 44 (*TIMM44*) was the only mitochondrial gene consistently over-expressed in the 3 comparisons with the highest over-expression in mosquitoes that survive CFP exposure compared to unselected (FC 18.7) but also against selected unexposed (FC 6.0) **(Data S3** to **S5)**.

A direct comparison of selected mosquitoes vs unselected (R_vs_S) revealed a striking down-regulation of major pyrethroid resistance genes. These include 35 down-regulated P450s, including *CYP6P3*, *CYP9K1*, *CYP6AA1, CYP6M2*, and 8 up-regulated P450s **(**Figure 1B and **Table S2)**; 16 down-regulated glutathione S-transferase genes, including *GSTe1 and GSTe2* (**Figure S2A**); ABC transporters [>20 down-regulated and 9 up-regulated (**Figure S2B**)], and cuticular proteins [78 down-regulated and 5 up-regulated (**Figure S2C**)] suggesting that mechanisms of resistance to CFP and pyrethroids might be contrasting **(Figure S2** and **Table S1)** as recently observed in the crop pest *T. urticae*.[13] This indicates that mosquitoes develop CFP resistance tandemly through a loss of pyrethroid resistance highlighting the need to maintain a pyrethroid selection in field populations to maximize CFP efficacy. Nevertheless, analysis of the R_vs_S comparison **(Data S2** and **Tables S1** and **S2)** revealed the over-expression of several genes known to be associated with insecticide resistance including ABC transporters (9 transcripts; 2.3<FC<5.7; **Figure S2B**), 4 alkaline phosphatases (with AGAP007300 with highest FC = 20.5), 8 carboxylesterases, and 8 cytochrome P450 (with *CYP4C26* as highest FC of 7.9). Three COEs exhibited high fold changes (FC), with *COEAE80* being the most prominent (FC = 67.1) (Figure 1D and **Table S1)**.

Gene Ontology enrichment analysis of over-transcribed genes in the CFP line showed no common pyrethroid resistance functions but mainly biological regulation. The down-regulated genes were enriched in energy production GO terms, suggesting that downregulation of certain metabolic processes may contribute to CFP resistance (**Figure S2, D** and **E**).

To detect potential genetic variants associated to CFP resistance, a genome-wide RNAseq-based variant calling was performed. Moreover, a principal component analysis (PCA) using genotype data encompassing the 3 chromosomes of *An. gambiae* was performed to investigate the impact of chlorfenapyr selection experiment at the genetic level. Overall, PCA showed three clusters on the five contigs except on the 3L chromosomal arm which indicated four groups as reflected by PCA from gene expression data (**Figure S3**). Polymorphism analysis led to the identification of 244,592 non-synonymous mutations across the five chromosomal arms (**Figure S2F** and **Data S10**).

An F_{ST} analysis was performed to detect SNPs exhibiting the highest genetic differentiation between selected and unselected samples (Figure 1F). When comparing mosquitoes selected that survived CFP exposure (R) to the unselected (S), the highest peak (F_{ST} ~ 0.24) was detected on chromosome 3R (~41Mbp) around several genes including cadherins (AGAP009715, AGAP009716 and AGAP009717) and odorant receptors (AGAP009718 and AGAP009719) which were not among the most over-expressed genes (Figure 1F). Another signal (F_{ST} ~ 0.20) appeared around the *Tep1* gene (AGAP010815) on chromosome 3L (~9Mbp). Similarly, an F_{ST} ~ 0.13 was noticed on chromosome X (~4.4Mbp) in a region containing odorant receptors (Or41 AGAP000226 and Or52 AGAP000230), netrin1 (AGAP000228), CREB (AGAP000237), the 3',5'-cyclic-nucleotide phosphodiesterase (AGAP000236) and histamine-gated chloride channel subunit (AGAP012975). No peak was observed around the top over-expressed genes (*cyclin B*, *CPR19*, *TIM44* and *HPX8*) except for the COEAE80 where a weak signal was detected (F_{ST} ~ 0.14) on chromosome 2L (~37Mbp). No clear differentiation was observed around the main pyrethroid resistance loci including the *CYP6*, *VGSC,* GTSs and *CYP9K1* (Figure 1F) contrasting with the comparison between CFP selected and parental line Mangoum (highly pyrethroid resistant strain) where strong signals were detected in these loci (*CYP6*: F_{ST} ~ 0.70, *VGSC*: F_{ST} ~ 0.70, GTSs: F_{ST} ~ 0.55 and *CYP9K1*: F_{ST} ~ 0.50) (**Figure S4A**). This aligns with the contrasting pattern observed in gene expression data where there was significant downregulation of major pyrethroid resistance genes (located on *CYP6, GSTs* and *CYP9K1* loci) in CFP line as compared to either the unselected line or the field parental line. Moreover, a Welch's t-test was performed to detect the most significant SNPs using the four replicates of each sample and the Log10 of P values were plotted on a Manhattan Plot (Figure 1G). Overall, most of the significant SNPs between R-S were synonymous mutations while the most significant non-synonymous mutations were detected on chromosome 3R, 2R and 2L including P537T (P = 1.90E-07) in the Methionine-tRNA ligase (AGAP007891), L1480V (P = 3.04E-07) in the vacuolar protein sorting

13 (AGAP005082) and S587Y (P = 1.18E-06) in the RIC3 domain-containing protein (AGAP005057) (Figure 1G, **Figure S4C** and **Data S11**). Other significant SNPs were detected in AGAP005471 (Q2244R, Q1831R, T4336A, T4224A, T3919A, T4031A and T3506A), AGAP001132 (Zinc finger protein 235, T176P), AGAP010727 (V39A) and AGAP012400 (G589C) (Figure 1G, **Figure S4C** and **Data S11**). The comparison between R and field parental strain yielded the A748S-AGAP000126 (6.44E-10) located on Chr X as the most significant non-synonymous mutation (**Figure S4, B** and **D** and **Data S11**). Indeed, the A748S was present at 98% in R as compared to 1% in the parental strain Mangoum. Other significant non-synonymous SNPs included A169E-AGAP008621 (1.53E-09), T52A-AGAP011334 (1.94E-09), D170H-AGAP008621 (1.97E-09) and V547I-AGAP029508 (5.15E-09) (**Figure S4, B** and **D** and **Data S11**). Almost all the amino-acid changes were present at high frequency in R ranging from 66-99% as compared to <11% in Mangoum population. However, some SNPs exhibited higher frequency in Mangoum strain as compared to R including E485D-AGAP029758 (99% vs 16%, P = 2.45E-08), V687L-AGAP029108 (99% vs 25%, P = 3.41E-08), T289A-AGAP011810 (97% vs 12%, P = 1.35E-07) and S344G-AGAP005922 (98% vs 25%, P = 4.60E-08) (**Figure S4, B** and **D** and **Data S11**).

Moreover, to detect potential SNPs associated with the over-expression observed in the RNAseq, a comparative analysis of the polymorphism pattern of over-expressed genes was performed. Four amino acid changes were identified in the most upregulated gene COEAE80 including A271T, I279V, E510D, A514V and A517V, with all mutations except E510D present relatively at similar frequency in unexposed and CFP survivors from the selected line (Figure 1E). E510D allele is present at 4% in the unexposed CFP selected and at 23% in CFP survivors from the same line suggestive of its potential role in CFP resistance. All these mutations above in COEAE80 were completely absent in the unselected line. A single mutation K177R in cyclin B (AGAP004963) was detected in all group except the susceptible strain Kisumu. Several SNPs were also detected in the translocase of inner mitochondrial membrane 44 gene AGAP008539 with the most prominent being the G323R exhibiting frequency of 58% in CFP survivors and 46% in unexposed selected line but absent in both parental colony from Mangoum and Unselected colony. The V288I was fixed in unselected and CFP selected strains while the Q77L was higher (88%) in the unexposed selected as compared to CFP survivors (64%) selected line. SNPs in the overexpressed heme peroxidase gene (HPX8) include S762A/T, K79R, S35A, P34L with similar allele frequencies ranging from 58 to 75% between CFP survivors and unexposed selected strain (Figure 1E).

Further attention was paid on missense mutations from genes which might be associated to metabolism of chlorfenapyr including detoxication genes (cytochrome P450s, glutathione-S-transferases, carboxylesterases), ATP and mitochondrial related genes involved in respiration function (Figure 1E and **Figure S5, A, B** and **C**). Looking at the ATP and Mitochondrial related genes (**Figure S5A**) revealed mutations with frequency of 0-8% in the unexposed selected strain and ≥15% in CFP survivors selected strain including AGAP008380 (K218Q/R/N), AGAP028189 (D543G, Q530H, P390A, L382I). In the CYP6 cluster located on 2R chromosomal arm known as the resistance to pyrethroid locus (rp1) (**Figure S5B**), most of the missense substitutions were present at high frequency in the parental strain Mangoum ranging from 76% to 100% particularly for the *CYP6P15P*, *CYP6P1*, *CYP6AD1*, *CYP6AA2*, *CYP6AA1* and *CYP6P3* genes. The E205D-CYP6P3 mutation recently associated to pyrethroid resistance[20] was high in the field parental strain (76%) but lower (<18%) in both unselected and CFP selected lines suggestive its opposite implication in CFP resistance. Indeed, gene expression data revealed downregulation of the CYP6P3, biomarker of pyrethroid resistance in CFP survivor mosquitoes and this gene has been shown to convert CFP to its toxic compound Tralopyril.[6] Other SNPs detected in several cuticular proteins and detox genes (ATP-biding cassettes and GSTs) are presented in the supplementary file (**Figure S6, B** and **C**).

The well-known pyrethroid resistance marker L995F in the voltage-gated sodium channel gene (VGSC) (**Figure S6A**) in *An. gambiae* was nearly fixed (96%) in the parental line but did not show a significant difference between CFP-selected and unselected samples.

PoolSeq whole genome association studies detect signatures of CFP resistance selection

Pooled whole genome sequencing of F_{12} hybrid mosquitoes was conducted to identify genetic variants driving CFP resistance. DNA pools, each comprising 50 mosquitoes were sequenced, including three from CFP-R resistant mosquitoes (surviving ≥60 min of CFP exposure), one from the CFP-susceptible mosquitoes (dying after ≤30 min) as well as the mosquitoes from F_6, F_9 and F_{12} in the CFP-selected line and the Kisumu susceptible lab strain. Sequencing depth varied from 27-76% (**Table S4).** Principal component analysis indicated distinct clustering based on phenotypes (**Figure S7**). The F_{ST} comparison of the mosquitoes from the CFP-selected line (CFP-R) (alive after exposure) to the dead and the susceptible lab-strain (Kisumu) mosquitoes identified genetic signals across all chromosomes with notable loci on CHR 2R (Figure 3A and **Figure S8A**). On CHR 2R, a locus containing insecticide resistance-related genes including *ABCC7*, histone methyltransferase (*ASHIL*), cuticular protein (*TWDL10*) and oxidation resistance protein (AGAP001751) were observed in both comparisons (F_{ST} alive_vs_dead = 0.028 and F_{ST} alive vs Kisumu = 0.365).

Another common peak (F_{ST} alive_vs dead = 0.017 and F_{ST} Alive_vs Kisumu = 0.24) was found in a region covering the *CYP6* cluster, and odorant binding protein 66 gene (*OBP66*). Genome-wide Fisher exact test confirmed these two peaks with p values as low as 4.37E-17 observed in the CYP6 cluster region (Figure 3B). Similarly, on CHR 2L, a common peak (F_{ST}_alive vs dead = 0.031 and F_{ST}_alive vs Kisumu = 0.199) at around 20Mb was identified containing detoxifying enzymes found within the *CYP4J*, *COEJHE genes* and cuticular protein (*CPR*) clusters as well as the E1A-binding protein p400 (AGAP006165) genes (P = 6.90E-08) (Figure 3, **A** and **B**). A single region containing the phosphoglucose isomerase gene (Pgi, AGAP012167) was found on CHR 3L with genome-wide significance (P = 7.89E-09). As the parental line was not sequenced due to unforeseen experimental constraints at the time of the study, generation F_6 mosquitoes were used as a pragmatic proxy for the parental susceptible line (less resistant generation). Same results as those with CFP_selF_{12} alive vs CFP_selF_{12} dead comparison were obtained when comparing F_{12} to F_6 mosquitoes, except for new peaks containing the 3',5'-cyclic-nucleotide phosphodiesterase (AGAP007163), mitochondrial uncoupling protein (AGAP009603) and CYP9K1 genes in CHR 2L, 3R and X respectively (Figure 3C and **Figure S8, B** to **D**). It is worth mentioning that contrary to our gene expression RNA-seq analysis, loci containing COEAE80 and Cyclin B were not detected as major peaks upon comparison of phenotype (dead vs alive) as well as inter-generation selected mosquitoes (Figure 3, **A** and **B**). However, such loci were identified with the Kisumu comparisons with F_{ST} peak of 0.266 and 0.2143, respectively (**Figure S8, A** and **E**). Common peaks on CHR 3R and CHR 3L contained genes related to odorant receptors and detoxifying enzymes.

A genome-wide analysis of nucleotide diversity and Tajima's D was performed to investigate genetic variations linked to phenotypic differences. Two regions on chromosome 2R (5-10Mb and 29-31Mb) exhibited reduced nucleotide diversity in the alive mosquitoes, with mean π values of 0.007 and 0.005, compared to 0.01 and 0.007 in the dead (**Figure S9, A** and **B**). A zoom into the 5-10Mb region referred to here as the oxidation resistance protein region portrayed further the reduction of nucleotide diversity, with CFP-alive mosquitoes having pi lower than 0.005 compared to the other phenotypes (Figure 2D). Moreover, negative Tajima's D values were observed in that region (Figure 2E), suggesting positive selection or population expansion. Surprisingly, a higher diversity was observed in alive mosquitoes relative to the other phenotypes (Dead, F_6 and F_{12}) on CHR 2L spanning the *COEAE80* region (Figure 2F and **Figure S5, C** and **D**).

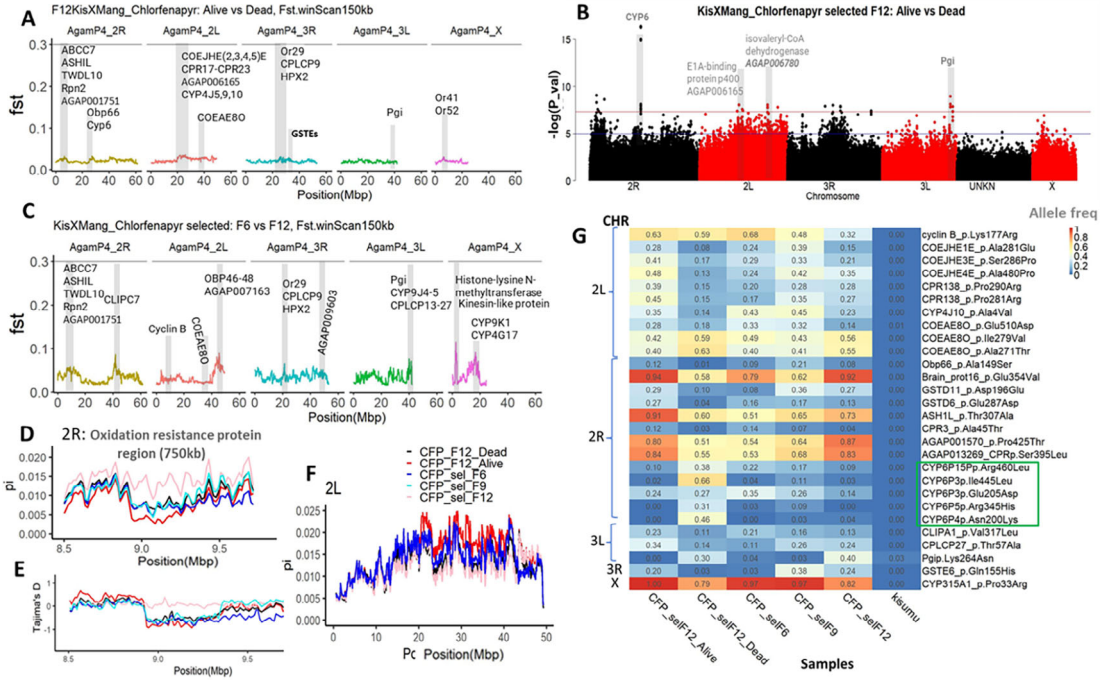

Figure 2. Pairwise F_{ST} comparison between different study populations and nucleotide diversity (pi), and Tajima's D along chromosomes. (**A**) F_{ST} CFP_selF_{12} alive versus CFP_selF_{12} dead. (**B**) Genome-wide Fisher exact test between CFP_selF_{12} alive versus CFP_selF_{12} dead. (**C**) F_{ST} CFP_selF_{12} versus CFP_selF_6. Gray bars represent the peaks (region of interest). (**D** and **E**) Zoom on a region (oxidation resistance protein) with reduced diversity on CHR 2R. (**F**) Nucleotide diversity on CHR 2L showing higher pi in CFP_selF_{12} alive. The F_{ST}, pi and Tajima's D values were calculated within a window of 150kb and 75kb window steps using winScan and F_{ST} per SNP generated in popoolation2. (**G**) Minor allele frequency of significant SNPs between different study populations, the green box on the heatmap delineates the CYP6 cluster genes.

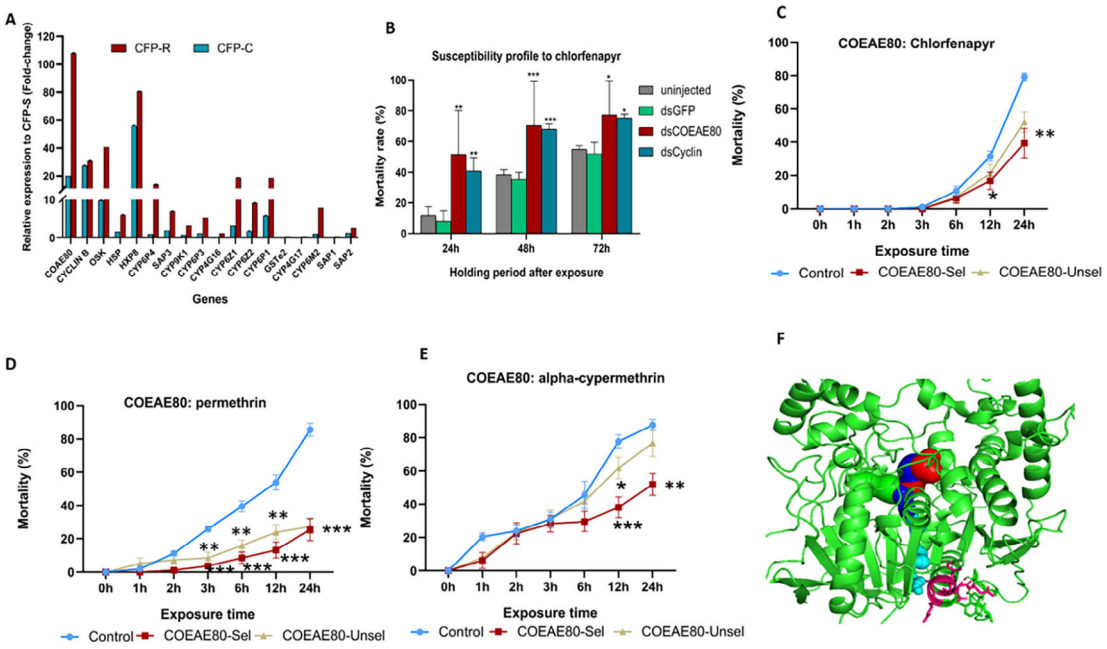

Figure 3. Functional validation of key candidate genes/genetic variants associated with chlorfenapyr resistance. (**A)** RT-qPCR to confirm overexpression of candidate genes confirming significant overexpression of *COEAE80* in CFP-R compared to CFP-S. (**B**) RNAi results after knockdown of the *COEAE80* (AGAP006700) and *cyclin B* (AGAP004963) confirming high implication to CFP resistance. (**C, D** and **E)** Mortality pattern of GAL4 x UAS-*COAE80* transgenic flies exposed to chlorfenapyr and pyrethroid (permethrin and alphacypermethrin) insecticides respectively. Asterisks indicate the difference between each ds-*COAE80*/GFP gene in comparison to ds-GFP control and un-injected mosquitoes and comparison between CFP-R (COEAE80-Sel), and CPF-S (COEAE80-Unsel) transgenic fly lines compared to the control (*P < 0.05, ** P < 0.01, *** P < 0.001). (**F**) 3D folding of *COEAE80* CFP-R model showing the access tunnels 1 (red), 2 (blue), 3 (green) and 4 (cyan). The predicted channel lining residues are in magenta and stick formats.

Additional regions of reduced diversity were identified on chromosomes 3L and X (**Figure S5, G** and **J**), associated with genes linked to CFP resistance. SNP analysis revealed non-synonymous mutations with higher frequencies in alive mosquitoes, including T307A in ASH1L (P < 0.0001) on CHR 2R. It is interesting to observe that non-synonymous mutations within the CYP6 cluster genes, such as CYP6P15P, CYP6P5, CYP6P4, and CYP6P3 were negatively associated with CFP resistance. Dead mosquitoes had significantly higher allele frequencies relative to their alive or resistant counterparts (P = 4.37E-17, Figure 3G). Another mutation K264N, in the phosphoglucose isomerase (Pgi) gene involved in energy production showed the same pattern as the CYP6 clusters. Candidate CFP-resistance mutations were also discovered in the carboxylesterase gene *COEAE80* with the E510D having higher frequency in alive (0.27) compared to dead (0.17, P = 0.22) and Kisumu (0.0056, P < 0.0001) (Figure 2G), confirming the RNA-seq results. The I279V had a slightly higher frequency in F_{12} progenies (0.56), compared to F_6 (0.49) and F_9 (0.43). Moreover, a significantly higher frequency was seen in alive mosquitoes (0.4) compared to Kisumu (P < 0.0001). A K177R variant in *Cyclin B* (AGAP004963) exhibited a similar association with CFP resistance as the I279V in *COEAE80.* Consequently, more emphasis was placed on *COEAE80* and *Cyclin B* (which were among the top upregulated candidate genes from the RNAseq analysis) for further analysis.

In-vivo and *In-silico* functional assays confirmed the implication of COEAE80 in chlorfenapyr resistance

RNAi-knockdown experiments, following confirmation of *COEAE80* overexpression in CFP-resistant *An. gambiae* mosquitoes via qRT-PCR (Figure 3A), validated its role in conferring CFP resistance. The results showed a significant increase in mortality (P < 0.0001) in mosquitoes injected with *dsCOEAE80 (*mortality rate at 72 h post-exposure to CFP 50 ug/ml = 77.3% ± 22.2), compared to mosquitoes injected with dsGFP (mortality = 51.9% ± 7.4 at 72 h post-exposure), and to those non-injected (mortality 54.9% ± 2.4 at 72 h post-exposure). Similar result was obtained for Cyclin B (Figure 3B). Transgenic *Drosophila melanogaster* expressing key alleles of recombinant *COEAE80* were generated and subsequently exposed to CFP to further validate its role in conferring CFP resistance. Bioassays performed with CFP revealed that flies expressing *COEAE80* alleles were significantly more resistant to CFP at 12 h and 24 h post-exposure compared to control flies (P = 0.002) (Figure 4C).

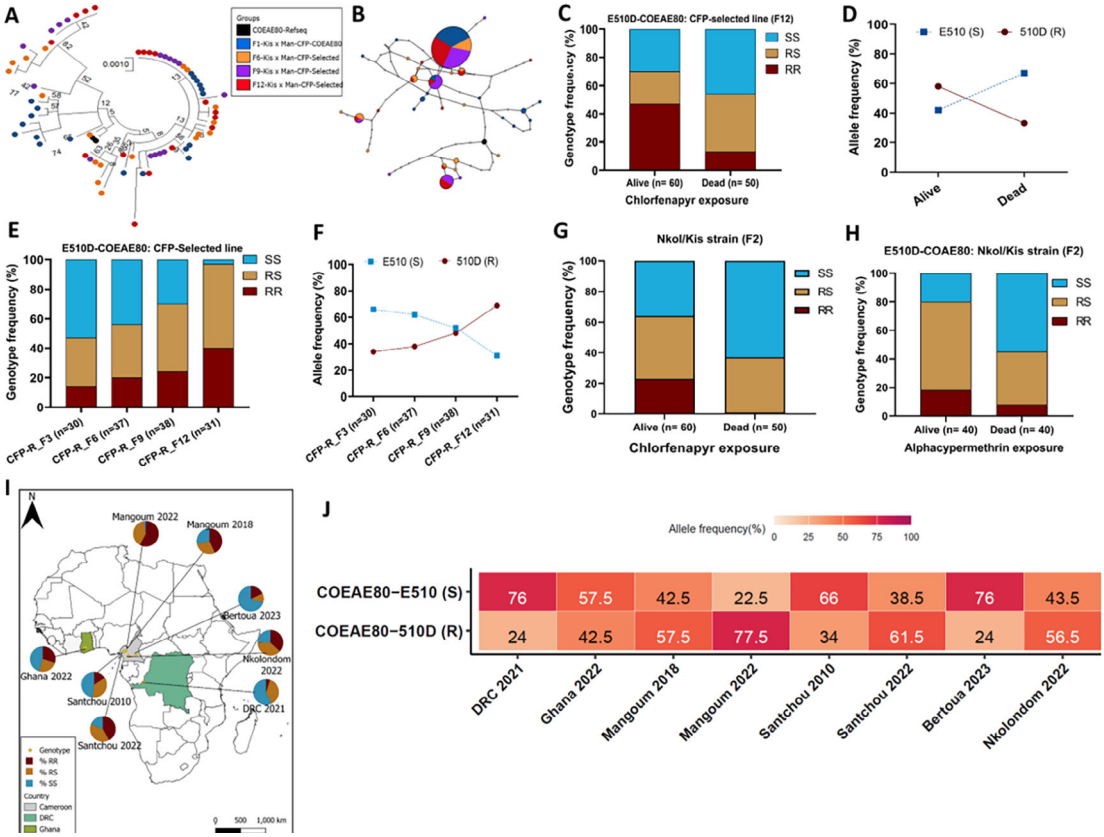

Figure 4. Impact of the newly detected marker of CFP resistance E510D-*COEAE80* on the ability of *An. gambiae* mosquitoes to withstand CFP exposure. (**A** and **B**) Genetic diversity assessment (Maximum likelihood tree and TCS haplotype network) of the *COEAE80* gene in relation to chlorfenapyr resistance selection. Numbers represent bootstrap values, which indicate the statistical support for each branch in the phylogenetic tree. (**C** and **D**) Genotype and allelic distribution of E510D-*COEAE80* marker respectively between highly susceptible (dead at 10 and 20 ug/ml of CFP) and highly resistant (alive at 50 and 100 ug/ml of CFP) mosquitoes from the CFP-selected line (F_{12}), 72h post-exposure to in CDC bottle bioassay. (**E** and **F)** Variation in genotype and allele frequency of E510D-*COEAE80* marker during the CFP selection process. (**G** and **H**) impact of E510D-*COEAE80* marker on the ability of *An. gambiae* from the field to withstand CFP and alphacypermethrin exposure. (**I**) Africa-wide distribution of the E510D-*COEAE80* CFP Marker in field (F_0) populations of *An. gambiae.* (**J**) Heatmap showing the temporal Cameroon-wide distribution of the allele frequency of the E510D-*COEAE80* CFP Marker in field (F_0) populations of *An. gambiae.*

Analysis of docking conformation of chlorfenapyr with COEAE80 revealed contrasting profiles between the CFP-R and CFP-S models. Within the CFP-S model chlorfenapyr docked with high total affinity (-7.9 kcal/mol, Figure 3F), in productive mode for an attack on the N-ethoxymethyl group nitrogen for N-dealkylation to generate the insecticidally toxic primary metabolite, tralopyril **(Figures S10** to **S12)**. Specifically, the catalytic triad S^{216} is hydrogen bonded to the ethoxy component of the N-ethoxymethyl group; a halogen bond was predicted between S^{242} and a fluorine atom on trifluoromethyl group; a pi-Cation interactions were observed between the fluorine atoms and the side chains of three residues (S^{242}, S^{217} and T^{247}); H^{468} pi stacked to the pyrrole ring; and a network of hydrophobic interactions was created by aliphatic (V^{355}, L^{306}) and aromatic (F^{307}, Y^{420}) towards chlorophenyl ring and the ethoxymethyl group.

In contrast, lower binding energy affinity was predicted for CFP-R models (e.g., -4.2 kcal/mol is the top score pose, **Figures S10** to **S12**). In all 30 docking poses analysed, chlorfenapyr docked unproductively, away from the active site gorge. Residues involved in interaction include E^{275}, E^{278} and V^{279} which are involved in hydrophobic interaction against the penultimate methyl moiety of the N-ethoxymethyl group; V^{279} involved in hydrophobic interaction against the chlorophenyl ring; H^{268} hydrogen bonded to the 3-carbonitrile group; and the same residue H^{268} involved in pi cation interaction and pi-pi stacking to the chlorophenyl ring.

Moreover, assessing the role of the E510D mutation in substrate channeling using CAVER identified a distinct tunnel for the CFP-R model, lined with critically important residue including 510D (Figure 3F). This suggests a nuanced impact of this mutation in substrate access/channeling.

The E510D-*COEAE80* strongly correlates with chlorfenapyr-resistance

Sequencing of the full-length *COEAE80* and *Cyclin B* genes revealed a greater reduced diversity for *COEAE80* in chlorfenapyr (CFP)-resistant mosquitoes, characterized by lower substitution sites and haplotype diversity (**Figure S13, B** and **C, Figure S14, A** to **E,** and **Table S5**). Phylogenetic analysis of *COEAE80* indicated clustering of resistant mosquitoes with a major haplotype, identifying four amino acid changes linked to CFP resistance: A271T, I279V, E331D, and E510D **(Figure S13, A** and **B)**. Notably, the frequency of E510D increased from 22.2% at F_6 to 25% at F_9 and 38.8% at F_{12} (Figure 4, **E** and **F**). This mutation was present in 62.5% of mosquitoes alive after CFP exposure compared to 27.7% of those that died ($P < 0.0001$). Genotyping of mosquitoes from the CFP-R strain showed a strong correlation between the E510D-*COEAE80* mutation and survival after CFP exposure, with homozygote resistant (RR) mosquitoes exhibiting significantly higher survival rates (OR = 6.3, $P < 0.0001$) (Figure 4, **C** and **D)**. In contrast, the I279V-COEAE80 mutation and the K117R-*cyclin B* showed no significant association with resistance (**Figure S14, A, B, D** and **E,** and **Table S5**). Additionally, genotyping revealed a gradual increase ($\chi^2 = 31.8$, $P < 0.0001$) in the frequency of the 510D-*COEAE80* resistance allele in the CFP-selected line from 32% at F_3 to 69% at F_{12} (Figure 4, **E** and **F)** whereas no consistent trend was seen for *Cyclin B* and other mutations (**Figure S15, C** and **F)**, establishing E510D-*COEAE80* as the best predictor of CFP resistance among tested markers.

The 510D-*COEAE80* CFP-resistance allele is detected across Africa

After detecting the presence of 510D-*COEAE80* mutant allele in different regions of sub-Saharan Africa (Figure 4I), its role in chlorfenapyr (CFP) and pyrethroid resistance was evaluated in a field population of *Anopheles gambiae* from Cameroon, specifically the Nkolondom/Kisumu F_2 hybrid strain. Spatio-temporal analysis revealed an increased frequency of this resistance allele in Santchou and Mangoum (Figure 4J), indicating a potential link to pyrethroid resistance. Genotyping results (Figure 4C) showed that homozygous resistant (RR) individuals for the E510D-*COEAE80* mutation had significant higher survival rates after CFP exposure compared to homozygous susceptible (SS) and

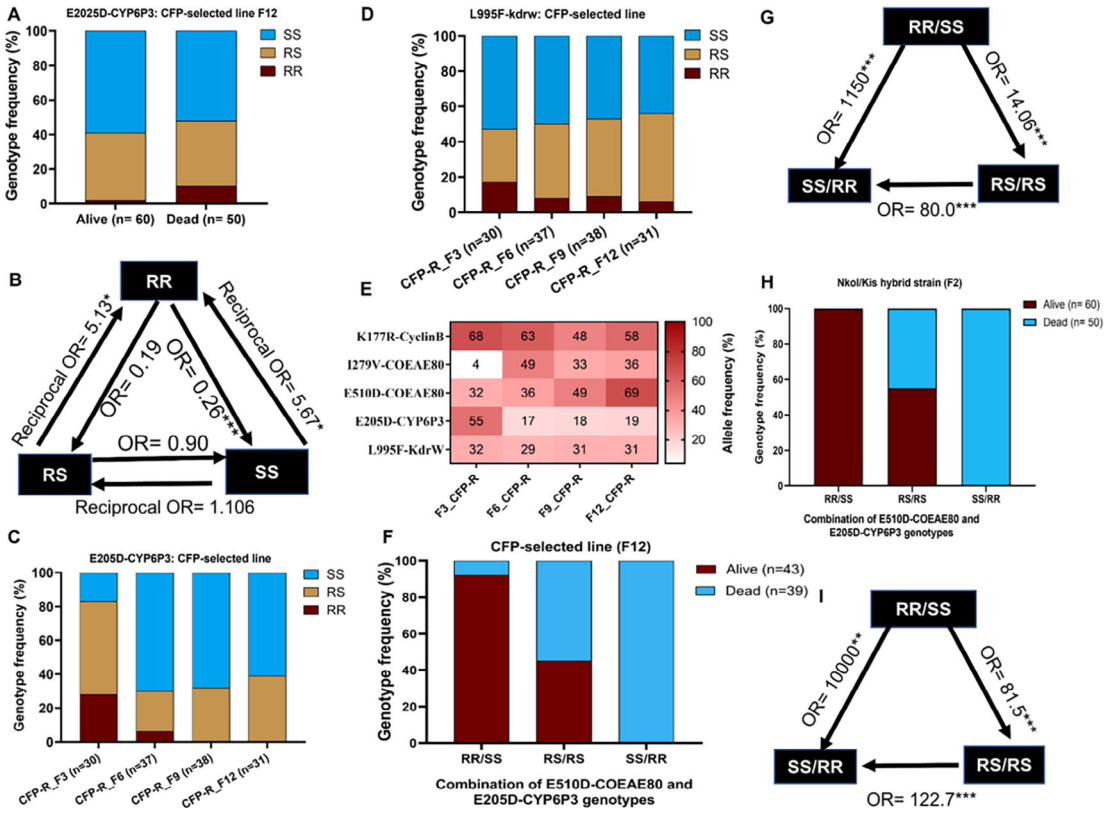

Figure 5. Contrasting impact between the E510D-*COEAE80* and the pyrethroid resistant markers on the ability of field *Anopheles gambiae* to survive chlorfenapyr exposure. (**A** and **B**) Genotype distribution of the pyrethroid resistant *marker* E205D-*CYP6P3* between dead and alive *An. gambiae* after exposure to CFP and the associated odds-ratio. (**C** and **D**) Variation in genotype frequency of E205D-*CYP6P3* and the L995F-*kdrw* markers during the CFP selection process. (**E** and **F**) Combined impact of E510D-*COEAE80* and E205D-*CYP6P3* markers on the ability of *An. gambiae* from the lab-selected strain to withstand CFP exposure. (**H** and **I)** Combined impact of E510D-*COEAE80* and E205D-*CYP6P3* markers on the ability of field *An. gambiae* to withstand CFP exposure.

heterozygous (RS) individuals, with odds ratios of 40.8 and 20.2, respectively ($P < 0.0001$). Additionally, further genotyping indicated that the E510D-COEAE80 marker also provides moderate resistance to type 2 (alphacypermethrin, Figure 4H) but not to type 1 (permethrin, **Figure S13, D** and **E**) and pyrethroids, highlighting its role in cross-resistance. Overall, this finding underscores the complex dynamics of resistance mechanisms in *An. gambiae* populations and emphasizes the need for strategic resistance management approaches.

Chlorfenapyr resistance involves a drastic reduction in the frequency of major pyrethroid resistance cytochrome P450 marker (E205D-*CYP6P3*)

Genotyping of mosquitoes from the chlorfenapyr-selected line revealed a contrasting relationship between pyrethroid and CFP resistance. Mosquitoes homozygous for the 205D-*CYP6P3* pyrethroid resistance allele had a significantly higher likelihood of dying after CFP exposure (OR = 0.26, $P < 0.0001$), compared to those with the susceptible E205-*CYP6P3* allele (Figure 5, **A** and **B, Figure S15H**). Accordingly, the frequency of the pyrethroid-resistant 205D-*CYP6P3* allele decreased from 55% to 19% during CFP selection (Figure 5, **C** and **E**) whereas no significant association was found with the L995F-*kdrw* target-site resistance marker (Figure 5, **D** and **E**). In addition, homozygous resistant mosquitoes (RR) for the E510D-*COEAE80* and homozygous susceptible (SS) for E205D-*CYP6P3* exhibited the highest survival rates after CFP exposure (OR = 11.50, $P < 0.0001$) (Figure 5, **F** and **G**). Interestingly, no survival occurred in mosquitoes that were SS or heterozygous for E510D-*COEAE80* and homozygous resistant for E205D-*CYP6P3*, indicating that while 510D-*COEAE80* confers resistance to CFP, the presence of 205D-*CYP6P3* likely counteract this effect. Field mosquitoes equally exhibited the highest survival rates when homozygous resistant for E510D-*COEAE80* and homozygous susceptible for E205D-*CYP6P3* and no survival was observed in mosquitoes that were either susceptible or heterozygous for E510D-*COEAE80* while being homozygous resistant for E205D-*CYP6P3* (Figure 5, **H** and **I**). This confirms that 510D-*COEAE80* confers resistance to CFP, while increased frequency of 205D-CYP6P3 may mitigate this effect.

Discussion

This study presents a comprehensive investigation of the molecular basis of chlorfenapyr resistance in the primary African malaria vector *Anopheles gambiae* detecting for the first-time major CFP resistance genes and revealing an antagonistic resistance route to that of pyrethroids. The design of a DNA-based molecular assay provides a reliable tool for early detection of chlorfenapyr resistance in the field to facilitate evidence-based control and resistance management, improving the capacity of malaria-endemic countries to combat malaria.

Signatures of CFP resistance is antagonistic to that of pyrethroid resistance

Our study provides the first laboratory evidence that *Anopheles* mosquitoes can develop resistance to chlorfenapyr (CFP), reinforcing recent field reports of reduced susceptibility in *An. gambiae* populations.[18] Remarkably, resistance emerged rapidly-within just 12 generations of CFP selection-mirroring patterns previously observed in agricultural pests such as in Bombyx mori[10] and *T. urticae*.[13] This swift adaptation highlights the potential risk of emerging resistance in areas with intensive CFP deployment, such as those using CFP-based nets,[21] underscoring the urgent need for proactive resistance surveillance and management strategies to preserve CFP's efficacy in malaria control.

The transcriptomic and genomic analyses revealed a strikingly opposite molecular signature to that seen to pyrethroids with the significant down-expression of major enzyme families associated with pyrethroid resistance, indicating that for CFP resistance to arise, mosquitoes must become susceptible to pyrethroids as shown previously.[17] This mechanism is noteworthy because most African mosquito populations are currently pyrethroid-resistant, and high P450 activity in these populations enhances CFP toxicity, suggesting that widespread pyrethroid resistance could delay the onset of CFP resistance.

In this study, we found that detoxification genes, particularly CYP450 enzymes, were downregulated in CFP-resistant mosquitoes. This downregulation is believed to prevent the bioactivation of chlorfenapyr into its toxic metabolite, tralopyril. In insects, chlorfenapyr metabolism has been shown to proceed primarily via CYP450-mediated N-ethoxymethyl dealkylation into insecticidally toxic primary metabolite, tralopyril,[22] including in *Anopheles* mosquitoes.[6,23] We interestingly revealed the key role played by carboxylesterases (*COEAE80*) in conferring CFP resistance in mosquitoes after *in-vivo* and *in-silico* functional validation. This is similar to the observation made previously that chlorfenapyr resistance is due to increased esterase activities in the housefly *Musca domestica,*[24] and the two-spotted spider mite, *T. urticae*.[25] The overexpression of carboxylesterases may provide an alternative detoxification route, compensating for the downregulation of P450s and potentially hydrolysing CFP or its metabolites before they exert toxic effects. Indeed, previous studies indicated that *CYP6P3*, *CYP9J5*, and *CYP9K1* in *An. gambiae* and *CYP9J32* in *Aedes aegypti* have great bio-activation potential of chlorfenapyr.[6] Similarly, heterologous analysis of chlorfenapyr metabolism in *An. funestus* indicated that the principal metabolite produced by *CYP6P9a* was tralopyril, the N-dealkylated insecticidal form that disrupts oxidative phosphorylation hence increasing mosquitoes susceptibility.[17] Our results suggest that the evolution of CFP resistance in mosquitoes is driven by a complex interplay between the downregulation

of P450-mediated bioactivation and the upregulation of carboxylesterase activity. This dual mechanism allows mosquitoes to evade the toxic effects of CFP, posing a significant challenge for vector control. Therefore, monitoring both P450 and carboxylesterase gene expression, as well as understanding their genetic regulation, will be critical for early detection and management of CFP resistance in the field. Integrating these molecular insights into resistance management strategies such as rotating insecticides with different modes of action and incorporating genomic surveillance will be essential to sustain the effectiveness of CFP-based interventions and safeguard public health gains in malaria-endemic regions.

E510D-*COEAE80*: a key player in chlorfenapyr resistance

So far, the possible genetic variation linked of resistance to CFP have not been well defined although multiple potential mechanisms have been described based on synergist and/or total enzyme assays. These include metabolic detoxification mediated by carboxyl/cholinesterases, glutathione S-transferases (GSTs) and cytochrome P450s (P450s), as well as decreased cuticular penetration.[8,10,13–15] These mechanisms can only explain a part of the resistant phenotype, and the precise underlying mechanisms had remained largely unknown. Genomic analyses further support the centrality of COEAE80 in CFP resistance. In this study, we successfully identified several genetic loci associated with chlorfenapyr resistance including genes related to metabolic detoxification and cuticular penetration. The presence of allelic variations in *COEAE80* (notably E510D) and cyclin B (K177R) was particularly noteworthy, as these genes were among the most overexpressed in resistant strains. The E510D mutation was significantly enriched in resistant mosquitoes and their frequencies increased across generations under selection pressure. Sanger sequencing validated the association of this variants with survival following CFP exposure, suggesting it may serve as reliable biomarkers for monitoring resistance evolution in the field.

While *COEAE80* stands out, CFP resistance is clearly polygenic. Signals of selection were also detected in loci encoding other detoxification enzymes, including cytochrome P450s (e.g., CYP325k1, CYP4J cluster), GSTs, and additional carboxylesterases (e.g., COEJHE, COE15O). It is worth mentioning that our poolseq analysis revealed mutations in the CYP6 cluster previously shown to confer resistance to pyrethroid to be negatively associated with CFP resistance, strengthening our RNAseq results. The over-expression of the translocase of inner mitochondrial membrane 44 (TIMM44), a mitochondrial gene, together with several missense mutations, could indicate that a more active mitochondrial function is equally contributing, at least indirectly, to CFP resistance. It has been suggested that the inner mitochondrial membrane translocase could contribute to insecticide resistance by regulating mitochondrial function known to be critical for detoxification and stress-responses which are energy-intensive processes.[26] Further investigation is warranted on the contribution of such mitochondrial gene knowing that CFP acts primarily through the disruption of ATP production by mitochondria.

Also, the detection of Histone methyltransferases both on CHR 2R (ASHIL) and CHR X (AGAP000042) could imply that CFP resistance in *An gambiae* could be under some degree of epigenetic control as reviewed previously by Mogilicherla and Roy in arthropods[27] and also suggested for pyrethroid resistance in *An. funestus.*[28] Such epigenetic modulation of insecticide resistance remains untested in *An. gambiae* and warrants further investigation. The presence of overexpressed *COEAE80* alongside these genes suggests a network of metabolic pathways working in concert to confer CFP resistance. Moreover, the detection of cuticular protein genes and odorant binding proteins indicates that penetration and behavioural resistance may further enhance the efficacy of metabolic mechanisms. However, higher overall nucleotide diversity in resistant populations suggests ongoing adaptation and the potential emergence of new resistance alleles, a pattern observed in other insecticide resistance studies.[28,29]

The prominence of *COEAE80* in both expression and selection analyses highlights its importance in CFP resistance and positions it as a promising candidate for molecular diagnostics. Targeted surveillance of *COEAE80* mutations and expression levels could provide early warning of emerging resistance, informing management strategies. However, the interplay with other metabolic and non-metabolic mechanisms underscores the need for integrated approaches to resistance monitoring and control, including the rotation of insecticides with different modes of action and the combination of chemical and non-chemical interventions.

In conclusion, while CFP resistance in *An. gambiae* is multifaceted, the evidence places COEAE80 at the forefront of metabolic adaptation, warranting further functional validation and field-based monitoring to sustain the efficacy of this critical intervention.

The 510D-*COEAE80* allele only confers CFP resistance in the absence of the P450 205D-*CYP6P3* pyrethroid resistance allele

A novel DNA-based assay was developed to track esterase-based metabolic resistance to chlorfenapyr (CFP) in *Anopheles gambiae* populations by exploiting allelic variations detected on *COEAE80* as done recently for

P450-based metabolic resistance to pyrethroids.[20,30,31] Interestingly, the highest survival rate after CFP exposure was observed in mosquitoes that were homozygous resistant for E510D-COEAE80 but homozygous susceptible for the E205D-*CYP6P3* P450 variant, supporting an antagonistic interaction between the two alleles and validating our Poolseq findings. The negative association with the E205D-*CYP6P3* pyrethroid resistance marker correlate well with the drastic down-regulation of P450 genes upon CFP exposure and with previous evidence that major pyrethroid resistance P450s bioactivate CFP to the more toxic tralopyril.[6,17] It therefore appears vital to combine CFP with pyrethroids to maximize the efficacy of these bed nets. Though not addressed in the current study, attention should be paid to genes associated with energy production, such as the phosphoglucose isomerase (Pgi), mitochondrial uncoupling protein which were found within genome-wide significant peaks (loci). It is important to recall that CFP mode of action involves mitochondrial disruption (uncoupler of oxidative phosphorylation). Mitochondria are the "powerhouses" of the cell, responsible for cellular respiration and the production of adenosine triphosphate (ATP), which is the primary energy currency for all cellular processes. Similar to CYP6 cluster, a mutation in Pgi was found negatively associated with CFP resistance, and this might suggest Pgi plays a supportive role like P450s in CFP resistance. This insight is also crucial for designing effective resistance management strategies, such as insecticide rotations or mixtures that exploit these antagonistic interactions.

Limitations of the study

In this study, the original parent colony was not sequenced due to unforeseen experimental constraints at the time of the study. In light of this, for our analysis, we utilized the F_6 colony as a pragmatic proxy for the parent strain. We do understand that this might have introduced a potential limitation to our study. Certain interest loci would have been missed as the F_6 colony was not made of a CFP naïve population but rather a CFP-selected one.

Conclusion

This study represents the first comprehensive examination of the molecular mechanisms underlying chlorfenapyr (CFP) resistance in mosquito species, highlighting the critical role of carboxylesterases. These enzymes, in conjunction with the downregulation of key metabolic pathways associated with CFP bioactivation particularly cytochrome P450s, drive CFP resistance. Our findings demonstrate that the overexpression of the carboxylesterase *COEAE80* and the selection of the 510D allele confer CFP resistance in both laboratory and field samples, with a more pronounced effect observed in mosquitoes possessing the susceptible P450 E205-*CYP6P3* allele. The development of a DNA-based assay will facilitate the early detection of CFP resistance Africa-wide. A key outcome of this study is the imperative need to always use CFP in combination with pyrethroids as resistance to pyrethroids increases susceptibility to CFP. Resistance to CFP will likely be rapidly selected and spread across Africa if CFP was to be applied without pyrethroids. Furthermore, the significant role of carboxylesterases suggests that the efficacy of CFP-treated nets could be improved by incorporating S,S,S-tributyl phosphorotrithioate (DEF) as a synergist, similar to the use of piperonyl butoxide (PBO) to inhibit P450 overexpression in pyrethroid-resistant mosquitoes.

Materials and methods

1-Mosquito collection

Anopheles gambiae mosquitoes were collected in May 2021 from Mangoum, located in the western region of Cameroon (5°29′09.2″ N 10°35′20.8″ E), and characterized by extensive agricultural practices. Mangoum has two rainy seasons (March-June and September-November) and two dry seasons (December-February and July-August) and *An. gambiae* s.s. is the predominant malaria mosquito in Mangoum with 4.10% *Plasmodium* infection rate.[32] This species is resistant to the four main classes of public health insecticides, with mortality rates <50% at 10x the pyrethroid discriminating doses.[32] Previous testing with CFP revealed that mosquitoes from this location exhibit a reduced susceptibility to this insecticide.[33]

2-Mosquito crossing and selection process

Crosses were performed between the Mangoum field mosquitoes and the KISUMU-S susceptible lab colony, and reared for 12 generations (F_{12}). To carry out this crossing, pupae from each strain were collected and placed individually in 15 ml falcon tubes. After emergence, males of the field strain were mixed in the same cage with females from the susceptible colony for random mating to generate the first generation of hybrids. At the 4th generation, a backcross was performed between the hybrid line and the parental line from Mangoum to re-introduce the field background. The first generation of the back-cross was divided into two distinct lines for selection. The first line (CFP-S) was maintained without selection and used as control for the selection experiment. The second line (CFP-R) was selected with sublethal dose of chlorfenapyr. This insecticide was obtained as a pure active ingredient from Sigma and diluted in 100% acetone, and 250 ml glass bottles were impregnated with 1 ml of insecticide solution as previously described.[33] Selection was carried out by introducing 20-25 non-blood fed female mosquitoes (2-5-day-old) into the insecticide-impregnated bottles and doses used for selection were initially calibrated in order to reach 60% mortality in the CFP-R line, as done previously by

Zoh *et al.*[34] Mortality rates were recorded after 72 h to account for the slower effect of CFP. Mosquitoes that survived were transferred into new cages and blood-fed to generate eggs for the next generation. Selection was performed every two generations until the 12th generation (F_{12}). The susceptibility profile was comparatively established between both lines at various generations and mosquitoes from F_{12} progeny were used for further transcriptomic and genomic studies.

3-Transcriptional profiling of genes associated with CFP resistance

3.1-RNA extraction, library preparation and sequencing: RNA-sequencing (RNA-seq) was performed using the F_{12} mosquitoes to establish the differential gene expression between mosquitoes that survived exposure to chlorfenapyr from the CFP-selected line (CFP-R), those unexposed from the selected line as control (CFP-C) and the non-selected line (CFP-S). In addition, the parental line from Mangoum (unexposed) and the susceptible lab strain KISUMU were also sequenced and included in the comparison. For each strain, four pools of 10 three-day-old, non-blood fed females were used. Total RNA was extracted from each pool separately using the Arcturus PicoPure RNA isolation kit (Life Technologies, Carlsbad, CA, USA). RNA quantification and quality check were verified using Qubit 4 fluorometer (Invitrogen^{TM}, Thermo fisher scientific) and TapeStation 4150 (Agilent technologies) respectively. Library preparation and sequencing were undertaken by Novogene (Cambridge, UK) following the protocol recently described.[35] After demultiplexing and quality check using FastQC, fastq files were loaded into Strand NGS V3.2 (Strand Life Sciences) and mapped against the reference genome downloaded from the Vectorbase (https://vectorbase.org/common/downloads/release-64/AgambiaePEST/fasta/data/VectorBase-64_AgambiaePEST_Genome.fasta) using standard parameters described previously.[34,36] Raw reads count table was obtained from bam files against the gff version of the reference genome AgamPEST64 using featureCounts.

3.2-Differential gene expression analysis (DEG): Differential transcription analysis was performed on all protein coding genes with normalization and quantification based on the DESeq algorithm.[37] Only the genes showing a coverage ≥ 10 reads/kb in all replicates of all conditions were kept. In total, 10 comparisons were computed to test for difference in gene expression (**Figure S1D**). Firstly, to account for differences in genetic background (field and lab), impact of lab selection experiment with or without CFP in transcription profile, comparisons were done between the field parental colony Mangoum (Man) and the other mosquito strain including Kisumu (Man vs. Kis), unselected line CFP-S (Man vs. CFP-S), both alive CFP-R and unexposed from CFP selected line (Man vs. CFP-R and Man vs. CFP-C respectively). Secondly, three comparisons were done between the susceptible lab strain Kisumu and the experimental lines (CFP-S vs. Kis, CFP-C vs. Kis, CFP-R vs. Kis) to detect genes involved in general stress response. Finally, to detect potential candidate genes involved in CFP resistance, we performed three additional comparisons: CFP-C vs. CFP-S, CFP-R vs. CFP-S and CFP-R vs. CFP-C, with the former being use for inducible gene expression. Genes in all comparisons versus the lab strain Kisumu were considered as differentially expressed if log2 fold changellog2FC | ≥ 1 and p-adjusted values ≤0.05 (false discovery rate FDR from the Benjamini–Hochberg method).[38] The cutoff for genes differentially expressed with the remaining comparisons was set atllog2FC | ≥ 0.58 and ≤FDR 0.05. All the comparisons were computed using one-way ANOVA followed by a tukey HSD test as described previously.[34,36]

3.3-Gene ontology (GO) terms enrichment: GO enrichment and KEGG[39] pathway enrichment analysis of DEGs were respectively performed using R based on the hypergeometric distribution. Genes significantly over- and under-transcribed from the comparison for detecting potential candidate genes described above were subjected to a Gene Ontology term (GO-term) enrichment analysis using the functional annotation tool DAVID (http://david.abcc.ncifcrf.gov).[40] Reference gene list consisted in the total genes detected by RNA-seq. Over- and under-expressed genes were considered separately and GO-terms showing a Fisher's Exact test P value < 0.05 were considered enriched as compared to the reference list.

3.4-Detection of single-nucleotide polymorphism: RNAseq-based variant calling was performed using the four biological replicates from all the mosquito population including the field parental strain, the lab susceptible strain Kisumu, the unselected line, both alive and unexposed from CFP selected colony. Single-nucleotide polymorphisms (SNPs) were called by comparing nucleotides across all populations at each genomic position to the reference genome AgamPEST64 using samtools mpileup and Varscan 2.[41] Alignments with mapping quality smaller than 10 were not included for variant calling. Variant calling parameters thresholds were a phred-scaled confidence score cut-off of 30 or above. This score represents the confidence in the variant call. Other criteria include a coverage greater than 10. Because of the nature of RNAseq, all indels were removed using vcftools. A SNP multi-sample report was generated, including the population's allele frequency. Samples containing at least 75% of the mutant allele at a defined position were considered homozygous mutant for an allele. Heterozygotes contained 25-75% of the mutant allele. For each variant, its SNP effect (nonsynonymous, synonymous, 5′ UTR, 3′ UTR etc.) and the affected transcripts were predicted using snpEff tool (Cingolani et al., 2012). After filtering the missense mutations, the average allele frequency from the four biological replicates for each population was calculated and visualised in R version 4.4.2 using dplyr and ggplot2 packages

respectively, then heatmap was generated to enable comparison between populations. In addition, to further evaluate the impact of CFP selection experiment at the genetic level, principal component analysis was computed with RNAseq-based variant calling using genotype data following the RNAseq-pop pipeline.[42]

3.5-Transcriptome-wide association study (TWAS)

Pairwise F_{ST} were computed using VCFtools v0.01.16 on the filtered vcf data as described previously.[43] Briefly, F_{ST} was calculated in windows of 300kb moving in average of 100kb steps using the script: vcftools --vcf "$VCF_FILE" --fst-window-size 300000 --fst-window-step 100000 --weir-fst-pop "$pop1" --weir-fst-pop "$pop2" --out "${base1}_${base2}_${SUFFIX}". The two populations to be compared were represented by pop1 and pop2. The resulting output file.windowed.weir.fst was visualised as moving averages using the R packages "tidyquant" (function "geom_ma"; ma_fun=SMA; n=12) and "ggplot2" in R v4.5.0.

Furthermore, to detect significant SNPs, a Welch's t-test was computed by comparing the mean allele frequency of the four replicates between two groups in R v4.5.0 using the package "matrixTests" (function "row_t_welch"). The resulting output file include statistic = t-value, p value = p-value of the test, estimate1 = mean of group 1, estimate2 = mean of group 2, difference = mean difference. The output was visualised on a Manhattan plot by plotting the Log10 of P values of each SNP using the R package ggmanh. The top 40 significant SNPs was plotted on a heatmap using the ggplot2 package.

3.6-Polymorphism analysis of candidate chlorfenapyr resistance genes: Particular attention was given to the most overexpressed CFP-resistance candidates genes, *COEAE80 and Cyclin B.* Polymorphisms in these genes were comparatively assessed between CFP-R, CFP-C, CFP-S, Mangoum and Kisumu by focusing primarily on non-synonymous SNPs. Each replicate was arbitrarily considered as an individual to facilitate the analysis. Data from the SNP multi-sample report was used to retrieve the polymorphisms observed in each sample and this information was transferred to the full length of each gene retrieved from Vectorbase. BioEdit was used to input various polymorphisms using an ambiguous letter to indicate heterozygote positions. Genetic diversity assessment was done using DnaSP V6.12.[44] The package TCS was used for haplotype network analysis. For phylogenetic tree construction, MEGA X[45] was used based on maximum likelihood method with 1000 bootstraps.

4- Quantitative reverse transcriptase PCR for key candidate genes

RNAseq expression patterns of some of the most over-expressed detoxification genes were validated by quantitative reverse transcriptase PCR (qRT-PCR), including *COEAE80 (AGAP006700), Cyclin B (AGAP004963), OSK (AGAP003545), HSP (AGAP002076), HXP8 (AGAP004038), and CYP4C26 (AGAP000192). Besides, expression levels of some known pyrethroid resistance genes, including CYP6P4, CYP6P3, CYP6P1, CYP6M2, CYP9K1, CYP6Z1, CYP6Z2, GSTe2, CYP4G16, CYP4G17, SAP1, SAP2, and SAP3 were also established by RT-qPCR.* Total RNA was extracted from 3 batches of 10 female mosquitoes for each strain using the picopure RNA extraction kit, as previously described.[46] The primers utilised are listed in **Data S1**. One microgram of RNA from each of the three biological replicates was used as a template for cDNA synthesis using the superscript III (Invitrogen) with oligo-dT20 and RNase H, following the manufacturer's instructions. The qRT-PCR amplification was performed following standard protocol after establishing the standard curves for each gene to assess PCR efficiency and quantitative differences between samples using serial dilution. The relative expression level and fold-change (FC) was calculated according the $2^{-\Delta\Delta CT}$ method[47] and compared between the two lines after normalisation with Ribosomal protein S7 (RSP7) and Elongation factor (EF).

5-Selection signatures associated with chlorfenapyr selection using Pool-seq Whole genome sequencing approach*:*

5.1- Experimental Procedures: Pools of 50 DNA equimolar samples from each line (CFP-R, CFP-C, CFP-S and Kisumu) were generated and RNAse A (Qiagen, UK) treated to get rid of RNA contaminants according to the manufacturers' instructions. Pooling was done as previously described by Kengne-Ouafo and Colleagues[48] and the library generation was carried out with a total of 1 µg DNA per sample using the Illumina NEBNext® Ultra™DNA Library Prep Kit (NEB, USA) according to the manufacturer's instructions (target size of 150bp). Libraries were sequenced on an Illumina NovaSeq, generating paired end fastq reads.

5.2- Sequence analysis: FastQC v0.11.5 was used to assess reads' quality of the raw Data and low-quality reads were trimmed with Trimmomatic V0.32 using the default parameters. Cleaned reads were mapped to the reference *Anopheles gambiae* genome version 67 using BWA mem (Version: 0.7.17). Duplicates were marked and removed from the mapped reads with the Picard tools and the coverage and depth were computed using the coverage option of the samtools package (version 1.13). Popoolation2 v. 1.201 was used to compute genetic differentiation per SNP between populations. The F_{ST} was computed per window of 150 kb and 75 kb step-size using WindowScanr (version 0.1). Genome-wide Fisher exact

test was used to validate F_{ST} peaks. Using Popoolation2-generated minor allele frequencies, the principal component analysis was done using ade4 and factoextra packages. Popoolation (v.1.2.2) was used to assess the genetic diversity in the regions of interest (regions surrounding the major peaks of the comparison between CFP-R and CFP-S) following the pipeline described by Kengne-Ouafo and Colleagues.[48] Briefly, we calculated Pi and Tajima's D across the entire genome using a window size of 150 kb and a step size of 75kb. We then focused on regions with reduced diversity genome-wide, analysing them in more detail with a window size of 40kb and a step size of 20 kb. Finally, we compared these results with the main peaks identified using popoolation2 F_{ST} analysis. To pinpoint non-synonymous mutations linked to the observed phenotype, VarScan.v2.3.9 was used for SNP calling with the default parameters. Then, annotation was performed with SnpEffect. Visualization was undertaken in the R environment with the ggplot2 package.

6- *In-vivo* functional validation of differentially expressed detoxification genes by RNAi

To further validate the role of *COEAE80* and *Cyclin B* in chlorfenapyr resistance, RNAi knockdown approach was also exploited. Gene-specific primers for double-stranded RNA (dsRNA) synthesis were designed with BLOCK-iT™ RNAi Designer (ThermoFisher, city, USA). The dsRNA was synthesised using an *in vitro* Transcription T7 Kit (for siRNA Synthesis) (Taktable ara Biotechnology, Dalian, China) following the manufacturer's instructions. The dsRNA of the green fluorescent protein gene (GFP) was also synthesised and utilised as a negative control. NanoDrop 2000 spectrophotometer was used to measure the concentration and the purity of dsRNA samples, and RNA quality was established by 2% agarose gel electrophoresis. The dsRNA samples were stored in -20°C until use. A total of 2 µg dsRNA was injected into 2–5-day-old female mosquitoes using a Nanoject II microinjector (Drummond Scientific, city, USA). The injected mosquitoes were used for susceptibility testing 24 h post-injection of dsRNA or dsGFP, using CDC bottles treated with 50 µg chlorfenapyr following the protocol described above. Following exposure, they were transferred to paper cups and supplied with 10% sugar then mortality was recorded up to 72 h post-exposure. Each RNAi treatment was replicated four times, and each replicate comprised 20-25 mosquitoes.

7-*In-vivo* functional validation of *COEAE80* using GAL4/UAS transgenic expression in Drosophila

7.1. Construction of transgenic flies

To assess whether the overexpression of the *An. gambiae COEAE80* gene alone could provide resistance to CFP and/or pyrethroids, transgenic *Drosophila melanogaster* expressing this gene were generated and subsequently exposed to CFP and pyrethroids to establish mortality rates. The *An. gambiae COEAE80* gene was amplified using primers containing NotI and KpnI restriction sites **(Data S1).** The PCR amplicons were purified and cloned into the pJET1.2 vector, followed by miniprepping. The predominant alleles were then digested from the pJET1.2 plasmids using NotI and KpnI enzymes (Fermentas, Burlington, Ontario, Canada) and ligated into the pre-digested pUASattB vector using the same restriction enzymes. These constructs were transformed into *E. coli* DHα cells (Invitrogen, Inchinnan Business Park, Paisley, UK), as previously described.[49] The recombinant constructs pUAS::COEAE80 were injected into the germline of *D. melanogaster* carrying the attP40 docking site on chromosome 2 (y1 w67c23; P (CaryP) attP40,1;2) using the PhiC31 system.[50] The injection of flies and balancing were performed by the Cambridge Fly Facility (https://www.flyfacility.gen.cam.ac.uk/). Ubiquitous expression of pUAS::COEAE80 in the transgenic flies was achieved by crossing them with the driver line Act5C-GAL4 strain (y1 w*; P (Act5C-GAL4-w) E1/CyO,1;2) (Bloomington Stock Center, IN, USA). Flies without the UAS insert (white eyes) were also crossed with the Act5C-GAL4 line to create a control line. The expression of *An. gambiae COEAE80* in the experimental flies was confirmed by semi-quantitative PCR using RNA extracted from F1 flies obtained from crossings of each transgenic line with Gal4-Actin 2, as previously described.[49]

7.2. Insecticides contact bioassays

To investigate the impact of overexpression of *COEAE80* in cross-insecticide resistance between CFP and pyrethroids, the F_1 progenies (2-4-day old females) overexpressing *An. gambiae COEAE80* were exposed to insecticides as previously carried out.[49,51] Briefly, the transgenic flies and the control flies were exposed for 24 h to CFP (10 µg/ml) and pyrethroids (permethrin (2%) and alpha-cypermethrin (0.007%)). Five replicates of 20 to 25 flies each were used for the bioassays, and the knockdown were scored after 1 h, 2 h, 3 h, 6 h, 12 h, and 24 h. Mortality and knockdown rates were compared between experimental and control groups using Student's t-test.

8- *In silico* modelling of candidate *COEAE80* protein variants and CFP docking simulations

8.1. Sequence characterization of An. gambiae COEAE80 and prediction of structurally conserved regions

To predict the folding pattern and role of candidate mutations (I279V and E510D) in the activity of *COEAE80* (AGAP006700), its amino acid sequences were compared with the sequences of the structurally resolved E3 alpha esterase (*LcαE7*) from the Australian sheep blow fly, *Lucilia cuprina.*[52] Three amino acid sequences were utilized for this

comparison: (i) two predominant sequences, linked with chlorfenapyr resistance, which were amplified from laboratory selected *An. gambiae* mosquitoes (CFP-R1 and CFP-R2), and one predominant sequence amplified from unselected mosquitoes (CFP-S, identical to the sequences amplified from Kisumu susceptible colony). Structurally conserved regions, including the highly conserved pentapeptide elbow residues, acyl binding pockets and oxyanion hole residues, as well as critical active site catalytic triad residues were predicted through sequence-to-sequence alignments using the CLC sequence viewer 7.0 (http://www.clcbio.com/).

8.2. Prediction of the role of COEAE80 mutations on chlorfenapyr resistance using homology modelling and docking simulations

To predict the folding patterns of *COEAE80*, homology models of the predominant sequences were created using the Modeller 10.5[53] with the crystal structure of *L. cuprina LcαE7* (PDB: 5CH3)[54] as a template. The 5CH3 shares overall 31.7%, 32.07% and 32.06% identity to CFP-R1, CFP-R2 and CFP-S sequences, respectively. A total of 20 models were generated for each sequence, and the models were assessed externally using Errat version 2[55] to identify the best models from statistical patterns of non-bonded interaction between different atom types. Virtual structure of chlorfenapyr (CID_91778) was retrieved from chemID plus (https://pubchem.ncbi.nlm.nih.gov/compound/91778). Docking simulations were carried out using the Achilles Blind Docking Server,[56] which uses Vina_vision – a customised version of Autodock Vina. For each ligand, 30 binding poses/clusters were generated and sorted according to binding energy and conformation in the model's active site. Figures were prepared using the PyMOL 2.4.[57] Non-bonded interactions were predicted using protein-ligand interaction profiler.[58]

8.3. Prediction of substrate access/product egress channels

To identify substrate access and/or product egress channels for CFP, comparative channels search was conducted using models generated from CFP-R and CFP-S *COEAE80* variants. Channel searches and calculations were conducted using the algorithm tool CAVER 3.1[59] PyMOL plug in, with minimum probe radius of 0.6, shell depth of 4, shell radius of 3, clustering threshold of 3.5, number of approximating balls of 12, maximum distance of 3Å, and desired radius of 5Å.

9- Polymorphism analysis of candidate CFP resistance genes between alive and mosquitoes post CFP-exposure

The entire genomic sequences of *COEAE80 (*2.0 kb) *and Cyclin B (*2.2 kb) were amplified and directly sequenced using 10 mosquitoes each from CFP-R alive and dead after exposure to CFP, the CFP-S unselected line, and the susceptible lab strain Kisumu, to detect the genetic diversity and haplotypes associated with CFP resistance. The internal primers utilized for this are listed in **Data S1**. Amplification and purification of PCR products were performed as previously described.[60] The DNA sequences were aligned using Bioedit for polymorphisms detection. Genetic diversity assessment was done using DnaSP V6.12.[44] The package TCS was used for haplotype network analysis. For phylogenetic tree construction, fasta sequences were aligned using mafft-7.029 with the auto option, MEGA X[45] was used for phylogenetic trees inference by maximum likelihood with 1000 bootstraps.

10- Design of diagnostic tool

Upon assessing the genetic diversity and function of the *COEAE80* and *Cyclin B* genes, SNPs in the coding regions (I279V, and E510D for *COEAE80* and K177R for *Cyclin B*) found to be associated with CFP resistance after RNA-seq and pool-seq were used for the development of LNA and allele-specific PCR-based diagnostic tools. Primers are summarised in **Data S1**. For LNA, the amplification was done in a final volume of 10 µl containing 1 µmole of each probe, 2 µmoles of each primer in 1× PrimeTime Master Mix (IDT) or 1× Luna Universal qPCR Master Mix (NEB) and 1 µl of genomic DNA. Amplification was achieved using the 2 fast step settings with a hold at 95°C for 10 min and 40 cycles of 95°C for 10s denaturation and 60°C for 45s extension. For the allele-specific PCR (AS-PCR) diagnostic assays**,** two pairs of primers were needed (two outer and two inner primers) as described previously.[61] Specific primers were designed manually to match the mutation, and an additional mismatched nucleotide was added in the 3rd nucleotide from the 3′ end of each inner primer to enhance the specificity. More details on the primer sequences are given in **Data S1**. PCR was carried out using 10 mM of each primer and 1µl of genomic DNA as template in 15 µl reactions containing 10X Kapa Taq buffer A, 0.2 mM dNTPs, 1.5 mM MgCl2, 1U Kapa Taq (Kapa biosystems). The cycle parameters were: 1 cycle at 95°C for 2 min; 30 cycles of 94°C for 30 s, 58°C for 30 s, 72°C for 1 min and then a final extension step at 72°C for 10 min. PCR products were separated on 2% agarose gel by electrophoresis. This assay allowed us to establish the correlation between the newly detected marker and resistance to CFP and pyrethroids

11- Geographic distribution of the markers in field *An. gambiae* samples across Africa

To determine the geographic distribution of the various mutations in field mosquitoes, archived F_0 *An gambiae* samples collected from different African countries (Ghana, Cameroon and the Democratic Republic of Congo (DRC)) were

genotyped using designed AS-PCR tool. Samples collected from 4 localities in Cameroon (Bertoua, Santchou, Mangoum, Nkolondom) were also used to assess the distribution of this marker in the country. An assessment of the temporal evolution of the allele was also performed by comparing samples from same location collected at different timepoints notably in Cameroon [Mangoum (2018 vs 2022) and Santchou (2010 vs 2022)] as previously done by Kengne-Ouafo *et al.*[20]

Consent for publication

All authors declare consent for publication.

Availability of Data and materials

All data generated or analyzed in this study are included in the article and its Additional files. The DNA sequencing data supporting the conclusions of this article are available in the ENA database, with accession number **PRJEB85924**. Supplemental files could be found here: https://doi.org/10.6084/m9.figshare.30453509.

References

1. Bhatt S, *et al.*: **The effect of malaria control on Plasmodium falciparum in Africa between 2000 and 2015.**
2. WHO: **World malaria report 2020: 20 years of global progress and challenges.** *World malaria report 2020: 20 years of global progress and challenges.* 2020; **299**.
3. Mosha JF, *et al.*: **Effectiveness and cost-effectiveness against malaria of three types of dual-active-ingredient long-lasting insecticidal nets (LLINs) compared with pyrethroid-only LLINs in Tanzania: a four-arm, cluster-randomised trial.** 2022; **399**: 1227–1241.
4. Accrombessi M, *et al.*: **Assessing the efficacy of two dual-active ingredients long-lasting insecticidal nets for the control of malaria transmitted by pyrethroid-resistant vectors in Benin: study protocol for a three-arm, single-blinded, parallel, cluster-randomized controlled trial.** 2021; **21**: 1–12.
5. Mbewe NJ, *et al.*: **Efficacy of bednets with dual insecticide-treated netting (Interceptor® G2) on side and roof panels against Anopheles arabiensis in north-eastern Tanzania.** 2022; **15**: 326.
6. Yunta C, *et al.*: **Chlorfenapyr metabolism by mosquito P450s associated with pyrethroid resistance identifies potential activation markers.** *Sci. Rep.* 2023; **13**: 14124. **PubMed Abstract** | **Publisher Full Text** | **Free Full Text**
7. Vandenhole M, *et al.*: **Contrasting roles of cytochrome P450s in amitraz and chlorfenapyr resistance in the crop pest Tetranychus urticae.** *Insect Biochem. Mol. Biol.* 2024; **164**: 104039. **PubMed Abstract** | **Publisher Full Text**
8. Van Leeuwen T, Van Pottelberge S, Tirry L: **Biochemical analysis of a chlorfenapyr-selected resistant strain of Tetranychus urticae Koch.** *Pest Manag. Sci.* 2006; **62**: 425–433. **PubMed Abstract** | **Publisher Full Text**
9. Van Leeuwen T, Stillatus V, Tirry L: **Genetic analysis and cross-resistance spectrum of a laboratory-selected chlorfenapyr resistant strain of two-spotted spider mite (Acari: Tetranychidae).** *Exp. Appl. Acarol.* 2004; **32**: 249–261. **PubMed Abstract** | **Publisher Full Text**
10. Shao Y, *et al.*: **Transcriptional response of detoxifying enzyme genes in Bombyx mori under chlorfenapyr exposure.** *Pestic. Biochem. Physiol.* 2021; **177**: 104899. **PubMed Abstract** | **Publisher Full Text**
11. Hollingworth RM, Gadelhak G: **Mechanisms of action and toxicity of new pesticides that disrupt oxidative phosphorylation.** 1998; **2**: 253–266.
12. Huang P, *et al.*: **A Comprehensive Review of the Current Knowledge of Chlorfenapyr: Synthesis, Mode of Action, Resistance, and Environmental Toxicology.** 2023; **28**: 7673.
13. Vandenhole M, *et al.*: **Contrasting roles of cytochrome P450s in amitraz and chlorfenapyr resistance in the crop pest Tetranychus urticae.** *Insect Biochem. Mol. Biol.* 2024; **164**: 104039. **PubMed Abstract** | **Publisher Full Text**
14. Van Leeuwen T, Stillatus V, Tirry L: **Genetic analysis and cross-resistance spectrum of a laboratory-selected chlorfenapyr resistant strain of two-spotted spider mite (Acari: Tetranychidae).** *Exp. Appl. Acarol.* 2004; **32**: 249–261. **PubMed Abstract** | **Publisher Full Text**
15. Uesugi R, Goka K, Osakabe M: **Genetic basis of resistances to chlorfenapyr and etoxazole in the two-spotted spider mite (Acari: Tetranychidae).** *J. Econ. Entomol.* 2002; **95**: 1267–1274. **PubMed Abstract** | **Publisher Full Text**
16. Shao Y, *et al.*: **Transcriptional response of detoxifying enzyme genes in Bombyx mori under chlorfenapyr exposure.** *Pestic. Biochem. Physiol.* 2021; **177**: 104899. **PubMed Abstract** | **Publisher Full Text**
17. Tchouakui M, *et al.*: **Substrate promiscuity of key resistance P450s confers clothianidin resistance while increasing chlorfenapyr potency in malaria vectors.** *Cell Rep.* 2024; **43**: 114566. **PubMed Abstract** | **Publisher Full Text** | **Free Full Text**
18. Tchouakui M, *et al.*: **Detection of a reduced susceptibility to chlorfenapyr in the malaria vector Anopheles gambiae contrasts with full susceptibility in Anopheles funestus across Africa.** *Sci. Rep.* 2023; **13**: 2363. **PubMed Abstract** | **Publisher Full Text** | **Free Full Text**
19. Xi J, *et al.*: **Elevated expression of esterase and cytochrome P450 are related with lambda-cyhalothrin resistance and lead to cross resistance in Aphis glycines Matsumura.** *Pestic. Biochem. Physiol.* 2015; **118**: 77–81. **PubMed Abstract** | **Publisher Full Text**
20. Kengne-Ouafo JA, *et al.*: **A single E205D allele of a key P450 CYP6P3 is driving metabolic pyrethroid resistance in the major African malaria vector Anopheles gambiae.** *bioRxiv.* 2024. 2024.2002.2018.580859
21. Patel P, Bagada A, Vadia N: **Management,, Treatments, Epidemiology and Current Trends in Malaria.** 2024; 261–282.
22. Black BC, Hollingworth RM, Ahammadsahib KI, *et al.*: **Insecticidal action and mitochondrial uncoupling activity of AC-303,630 and related halogenated pyrroles.** *Pestic. Biochem. Physiol.* 1994; **50**: 115–128. **Publisher Full Text**
23. Ibrahim SS, *et al.*: **Functional Validation of Endogenous Redox Partner Cytochrome P450 Reductase Reveals the Key P450s CYP6P9a/-b as Broad Substrate Metabolizers Conferring Cross-Resistance to Different Insecticide Classes in Anopheles funestus.** *Int. J. Mol. Sci.* 2024; **25**. **PubMed Abstract** | **Publisher Full Text** | **Free Full Text**
24. Kinareikina A, Silivanova E: **Impact of Insecticides at Sublethal Concentrations on the Enzyme Activities in Adult Musca domestica L.** *Toxics.* 2023; **11**. **PubMed Abstract** | **Publisher Full Text** | **Free Full Text**
25. Van Leeuwen T, Van Pottelberge S, Tirry L: **Comparative acaricide susceptibility and detoxifying enzyme activities in field-collected resistant and susceptible strains of Tetranychus urticae.** *Pest Manag. Sci.* 2005; **61**: 499–507. **PubMed Abstract** | **Publisher Full Text**
26. Lubawy J, Chowański S, Adamski Z, *et al.*: **Mitochondria as a target and central hub of energy division during cold stress in insects.** *Front. Zool.* 2022; **19**: 1. **PubMed Abstract** | **Publisher Full Text** | **Free Full Text**
27. Mogilicherla K, Roy A: **Epigenetic regulations as drivers of insecticide resistance and resilience to climate change in arthropod pests.** *Front. Genet.* 2022; **13**: 1044980.
28. Gadji M, *et al.*: **Genomic drivers of pyrethroid resistance escalation in the malaria vector Anopheles funestus across Africa [version 1].** *VeriXiv.* 2025; **2**.

29. C. The Anopheles gambiae Genomes, *et al.*: **Genetic diversity of the African malaria vector Anopheles gambiae.** *Nature.* 2017; **552**: 96.

30. Weedall GD, *et al.*: **A cytochrome P450 allele confers pyrethroid resistance on a major African malaria vector, reducing insecticide-treated bednet efficacy.** *Sci. Transl. Med.* 2019; **11**. **PubMed Abstract** | **Publisher Full Text**

31. Mugenzi LMJ, *et al.*: **A 6.5-kb intergenic structural variation enhances P450-mediated resistance to pyrethroids in malaria vectors lowering bed net efficacy.** *Mol. Ecol.* 2020; **29**: 4395–4411. **PubMed Abstract** | **Publisher Full Text**

32. Tepa A, *et al.*: **Molecular Drivers of Multiple and Elevated Resistance to Insecticides in a Population of the Malaria Vector Anopheles gambiae in Agriculture Hotspot of West Cameroon.** *Genes.* 2022; **13**: 1206. **PubMed Abstract** | **Publisher Full Text** | **Free Full Text**

33. Tchouakui M, *et al.*: **Detection of a reduced susceptibility to chlorfenapyr in the malaria vector Anopheles gambiae contrasts with full susceptibility in Anopheles funestus across Africa.** *Sci. Rep.* 2023; **13**: 2363. **PubMed Abstract** | **Publisher Full Text** | **Free Full Text**

34. Zoh MG, *et al.*: **Experimental evolution supports the potential of neonicotinoid-pyrethroid combination for managing insecticide resistance in malaria vectors.** 2021; **11**: 19501.

35. Weedall GD, *et al.*: **A cytochrome P450 allele confers pyrethroid resistance on a major African malaria vector, reducing insecticide-treated bednet efficacy.** *Sci. Transl. Med.* 2019; **11**. **PubMed Abstract** | **Publisher Full Text**

36. Wondji CS, Hearn J, Irving H, *et al.*: **RNAseq-based gene expression profiling of the Anopheles funestus pyrethroid-resistant strain FUMOZ highlights the predominant role of the duplicated CYP6P9a/b cytochrome P450s.** 2022; **12**: jkab352.

37. Anders S, Huber WJNP: **Differential expression analysis for sequence count data.** 2010; 1–1.

38. Benjamini Y, Hochberg Y: **Controlling the false discovery rate: a practical and powerful approach to multiple testing.** 1995; **57**: 289–300.

39. Kanehisa M, *et al.*: **KEGG for linking genomes to life and the environment.** 2007; **36**: D480–D484.

40. Huang DW, Sherman BT, Lempicki RA: **Bioinformatics enrichment tools: paths toward the comprehensive functional analysis of large gene lists.** 2009; **37**: 1–13.

41. Koboldt DC, *et al.*: **VarScan 2: somatic mutation and copy number alteration discovery in cancer by exome sequencing.** *Genome Res.* 2012; **22**: 568–576. **PubMed Abstract** | **Publisher Full Text** | **Free Full Text**

42. Nagi SC, Oruni A, Weetman D, *et al.*: **RNA-Seq-Pop: Exploiting the sequence in RNA sequencing-A Snakemake workflow reveals patterns of insecticide resistance in the malaria vector Anopheles gambiae.** *Mol. Ecol. Resour.* 2023; **23**: 946–961. **PubMed Abstract** | **Publisher Full Text** | **Free Full Text**

43. Schmidt TL, *et al.*: **Global, asynchronous partial sweeps at multiple insecticide resistance genes in Aedes mosquitoes.** *Nat. Commun.* 2024; **15**: 6251. **PubMed Abstract** | **Publisher Full Text** | **Free Full Text**

44. Rozas J, *et al.*: **DnaSP 6: DNA Sequence Polymorphism Analysis of Large Data Sets.** *Mol. Biol. Evol.* 2017; **34**: 3299–3302. **PubMed Abstract** | **Publisher Full Text**

45. Kumar S, Stecher G, Li M, *et al.*: **MEGA X: Molecular Evolutionary Genetics Analysis across Computing Platforms.** *Mol. Biol. Evol.* 2018; **35**: 1547–1549. **PubMed Abstract** | **Publisher Full Text** | **Free Full Text**

46. Riveron JM, *et al.*: **Directionally selected cytochrome P450 alleles are driving the spread of pyrethroid resistance in the major malaria vector Anopheles funestus.** 2013; **110**: 252–257.

47. Schmittgen TD, Livak KJ: **Analyzing real-time PCR data by the comparative CT method.** *Nat. Protoc.* 2008; **3**: 1101–1108. **Publisher Full Text**

48. Kengne-Ouafo JA, *et al.*: **A single E205D allele of a key P450 *CYP6P3* is driving metabolic pyrethroid resistance in the major African malaria vector *Anopheles gambiae.*** *bioRxiv.* 2024. 2024.2002.2018.580859.

49. Riveron JM, *et al.*: **A single mutation in the GSTe2 gene allows tracking of metabolically based insecticide resistance in a major malaria vector.** *Genome Biol.* 2014; **15**: 1–20.

50. Markstein M, Pitsouli C, Villalta C, *et al.*: **Exploiting position effects and the gypsy retrovirus insulator to engineer precisely expressed transgenes.** *Nat. Genet.* 2008; **40**: 476–483. **PubMed Abstract** | **Publisher Full Text** | **Free Full Text**

51. Tchouakui M, *et al.*: **Substrate promiscuity of key resistance P450s confers clothianidin resistance while increasing chlorfenapyr potency in malaria vectors.** *Cell Rep.* 2024; **43**: 114566. **PubMed Abstract** | **Publisher Full Text** | **Free Full Text**

52. Correy GJ, *et al.*: **Mapping the Accessible Conformational Landscape of an Insect Carboxylesterase Using Conformational Ensemble Analysis and Kinetic Crystallography.** *Structure.* 2016; **24**: 977–987. **PubMed Abstract** | **Publisher Full Text**

53. Webb B, Sali A: **Comparative Protein Structure Modeling Using MODELLER.** *Curr. Protoc. Bioinformatics.* 2016; **54**: 5 6 1–5 6 37. **Publisher Full Text**

54. Correy GJ, *et al.*: **Mapping the Accessible Conformational Landscape of an Insect Carboxylesterase Using Conformational Ensemble Analysis and Kinetic Crystallography.** *Structure.* 2016; **24**: 977–987. **PubMed Abstract** | **Publisher Full Text**

55. Colovos C, Yeates TO: **Verification of protein structures: patterns of nonbonded atomic interactions.** *Protein science: a publication of the Protein Society.* 1993; **2**: 1511–1519. **PubMed Abstract** | **Publisher Full Text** | **Free Full Text**

56. Sanchez-Linares I, Perez-Sanchez H, Cecilia JM, *et al.*: **High-Throughput parallel blind Virtual Screening using BINDSURF.** *BMC bioinformatics.* 2012; **13**: S13. **Publisher Full Text**

57. DeLano WL: **The PyMOL Molecular Graphics System.** 2004.

58. Salentin S, Schreiber S, Haupt VJ, *et al.*: **PLIP: fully automated protein-ligand interaction profiler.** *Nucleic Acids Res.* 2015; **43**: W443–W447. **PubMed Abstract** | **Publisher Full Text** | **Free Full Text**

59. Chovancova E, *et al.*: **CAVER 3.0: a tool for the analysis of transport pathways in dynamic protein structures.** *PLoS Comput. Biol.* 2012; **8**: e1002708. **PubMed Abstract** | **Publisher Full Text** | **Free Full Text**

60. Barnes KG, *et al.*: **Genomic footprints of selective sweeps from metabolic resistance to pyrethroids in African malaria vectors are driven by scale up of insecticide-based vector control.** 2017; **13**: e1006539.

61. Tchouakui M, *et al.*: **A marker of glutathione S-transferase-mediated resistance to insecticides is associated with higher Plasmodium infection in the African malaria vector Anopheles funestus.** 2019; **9**: 5772.